A microtubule-binding myosin required for nuclear anchoring and spindle assembly

Kari L. Weber[1]*, Anna M. Sokac[1,2]*, Jonathan S. Berg[3], Richard E. Cheney[3] & William M. Bement[1,2]

[1]*Department of Zoology,* [2]*Program in Cellular and Molecular Biology, University of Wisconsin, Madison, Madison, Wisconsin 53706, USA*
[3]*Department of Cell and Molecular Physiology, University of North Carolina, Chapel Hill, Chapel Hill, North Carolina 27599, USA*

* Present addresses: Department of Cell Biology, CB163, The Scripps Research Institute, 10550 N. Torrey Pines Road, La Jolla, California 92037, USA (K.L.W.); Department of Molecular Biology, Princeton University, Washington Road, Princeton, New Jersey 08544, USA (A.M.S.)

Proper spindle positioning and orientation are essential for asymmetric cell division and require microtubule–actin filament (F-actin) interactions in many systems[1,2]. Such interactions are particularly important in meiosis[3], where they mediate nuclear anchoring[4–6], as well as meiotic spindle assembly and rotation[7,8], two processes required for asymmetric cell division. Myosin-10 proteins are phosphoinositide-binding[9], actin-based motors that contain carboxy-terminal MyTH4 and FERM domains of unknown function[10]. Here we show that *Xenopus laevis* myosin-10 (Myo10) associates with microtubules *in vitro* and *in vivo*, and is concentrated at the point where the meiotic spindle contacts the F-actin-rich cortex. Microtubule association is mediated by the MyTH4-FERM domains, which bind directly to purified microtubules. Disruption of Myo10 function disrupts nuclear anchoring, spindle assembly and spindle–F-actin association. Thus, this myosin has a novel and critically important role during meiosis in integrating the F-actin and microtubule cytoskeletons.

Microtubule–F-actin interactions are essential for a broad variety of basic biological processes that require polarized distribution of cellular components[2]. Mitotic spindle positioning in yeast, for example, is critically dependent on physical linkages between microtubules and cortical F-actin[1]. Microtubule–F-actin interactions are particularly important in oogenesis, which entails anchoring and translocation of microtubule-based structures within a comparatively large cell volume[3]. For example, the oocyte nucleus (germinal vesicle) is anchored by microtubules that extend from the nucleus to the F-actin-rich cortex[4–6], whereas proper meiotic spindle assembly and/or targeting to the plasma membrane are F-actin dependent[3,7,8,11]. Further, the site of asymmetric spindle anchoring at the oocyte cortex is overlaid by a cap of high F-actin density in mammals[8,11], amphibians[7] and invertebrates[12,13]; this cap is thought to anchor the spindle at the cortex through interaction with microtubules[3,7,8,11]. At present, however, the molecular mechanisms that couple microtubules to F-actin during oogenesis are unknown.

Xenopus Myo10 was identified in a polymerase chain reaction

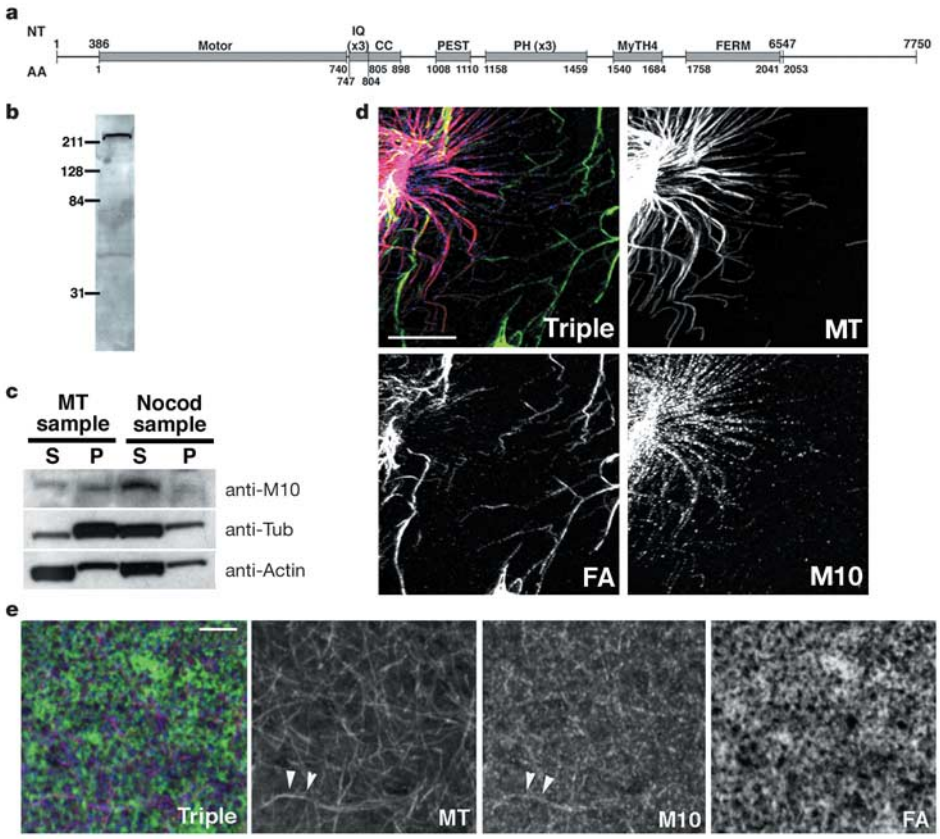

Figure 1 Myo10 associates with microtubules *in vitro* and *in vivo*. **a**, Domain organization of Myo10. **b**, Myo10 antibody recognizes single protein of ~230 kDa in egg extract immunoblot. **c**, Microtubule (P, pellet) and supernatant fractions (S) from egg extracts induced to (MT sample) or prevented from (Nocod sample) polymerizing microtubules (see Methods). Immunoblotting with antibodies to Myo10 (M10), tubulin (Tub) or actin (Actin) shows Myo10 cofractionates with microtubules but not actin filaments. **d**, Myo10 (M10, blue) immunolocalizes with aster microtubules (MT, red) but much less with F-actin (FA, green) in extracts. Scale bar, 30 μm. **e**, Myo10 also colocalizes with microtubules in intact eggs (arrowheads). Antibodies the same as in **d**. Scale bar, 20 μm.

©2004 Nature Publishing Group

(PCR) screen for myosins expressed in oocytes. Although myosins are best known as F-actin-based motors[14], we characterized Myo10 as a potential microtubule–F-actin linker in oocytes, based on its primary structure. That is, this unconventional vertebrate myosin contains a MyTH4 domain in its C-terminal tail[10], and the MyTH4 domain of an *Arabidopsis* kinesin-like protein was previously shown to bind microtubules[15]. The complete coding sequence of Myo10 was obtained (Fig. 1a; Supplementary Fig. S1) and polyclonal antibodies (directed against a small region in the actin-based motor 'head' region) were generated and affinity purified (Fig. 1b). Consistent with potential microtubule-binding, Myo10 co-sedimented with microtubules (Fig. 1c) and colocalized with microtubules in *Xenopus* egg extracts (Fig. 1d) and in intact *Xenopus* eggs (Fig. 1e). The observed immunolocalization of Myo10 on microtubules was specific and independent of F-actin (Supplementary Fig. S2), as expected if Myo10 bound directly to microtubules rather than associating indirectly through actin binding.

Myo10 showed a striking colocalization with meiotic spindle microtubules (Fig. 2). Specifically, Myo10 concentrated in the region where the spindle contacted the cortex (Fig. 2a, b), and on microtubules that extended upward from the spindle into the cortex, similar to guy wires (Fig. 2c, d). F-actin also colocalized with the spindle, both in the cortical cap and the interior of the spindle. Although some overlap of Myo10 and F-actin staining was observed, Myo10 was most abundant in the outer regions of the spindle and the cap, whereas F-actin was most abundant on the interior regions of the cap and the spindle (Fig. 2).

To determine the minimal region of Myo10 sufficient for microtubule association, a series of enhanced green fluorescent protein (eGFP)–Myo10 truncation constructs were expressed in oocytes by messenger RNA injection (Fig. 3a). Co-sedimentation analysis showed that the MyTH4-FERM domain cassette was sufficient to confer microtubule association (Fig. 3b). The association was independent of F-actin, as demonstrated by pretreating oocytes with latrunculin (Supplementary Fig. S3). To further dissect the region of Myo10 required for microtubule association and to determine whether microtubule binding was direct, we sought to express Myo10 tail constructs in bacteria. However, these efforts were frustrated by insolubility and instability of the expressed constructs. As an alternative approach, reticulocyte lysate was programmed with mRNA encoding eGFP alone or eGFP fused to MyTH4, FERM or the MyTH4-FERM cassette. After expression, lysate was combined with pure microtubules and analysed by co-sedimentation. Neither eGFP alone nor eGFP–FERM pelleted with microtubules, whereas eGFP–MyTH4 showed modest co-pelleting and eGFP–MyTH4-FERM showed significant co-pelleting (Fig. 3c), demonstrating that the MyTH4-FERM cassette was sufficient for microtubule association.

Because it could be argued that a component of the reticulocyte lysate was responsible for linking the MyTH4-FERM cassette to microtubules, mRNA encoding glutathione *S*-transferase (GST) alone or GST–MyTH4-FERM was injected into oocytes, and after translation, purified through gluthathione affinity (Supplementary Fig. S4). GST–MyTH4-FERM pelleted in the presence, but not the absence of microtubules, whereas GST alone did not pellet in the presence of microtubules (Fig. 3d). Thus, the MyTH4-FERM domain cassette of Myo10 binds directly to microtubules.

To assess the *in vivo* role of Myo10, oocytes were injected with mRNA encoding truncated proteins consisting of the pleckstrin homology (PH), MyTH4 and FERM domains fused to either eGFP or GST. Tail truncates function as dominant negatives for unconventional myosins in general[16] and more specifically, for myosin-10 in phagocytosis[17]. Both eGFP–Myo10 tail (Fig. 4a, b) and GST–Myo10 tail (data not shown) resulted in displacement of the oocyte

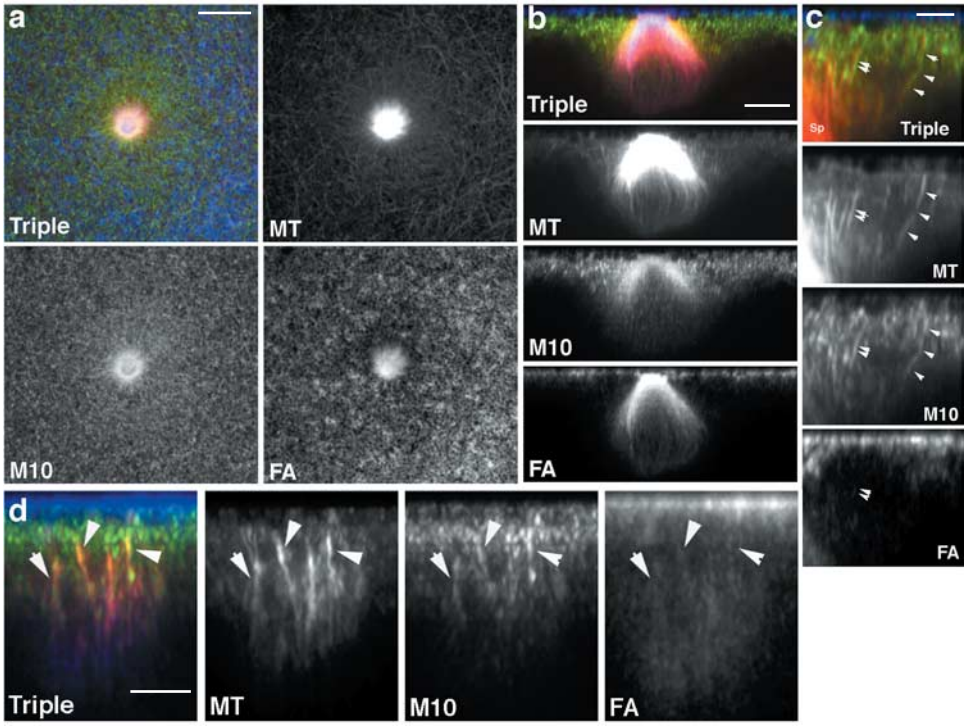

Figure 2 Myo10 localizes to meiotic spindles. **a**, Surface view shows colocalization of Myo10 (M10, green) and F-actin (FA, blue) with meiotic spindle (MT, red). Scale bar, 30 μm. **b**, Z-section shows that Myo10 and F-actin have overlapping but distinct distributions on the spindle with Myo10 predominantly around the outside and F-actin on the inside of the spindle. Scale bar, 15 μm. **c**, High magnification Z-section shows tracks of Myo10 on microtubules that extend upward from the spindle (sp) to the cortex (arrowheads). Tracks both with (double arrowheads) and without (single arrowheads) associated F-actin are seen. Scale bar, 5 μm. **d**, Grazing view of spindle shows Myo10 concentrated on spindle microtubules extending into the cortex (arrowheads). Scale bar, 5 μm.

©2004 Nature Publishing Group

nucleus (germinal vesicle) from its normal site of asymmetric localization in the animal hemisphere to the cortex, as shown by a large white spot at the animal pole. Consistent with results from other systems[17], displacement required the entire tail. The specificity of this effect was demonstrated by the fact that co-expression of eGFP–full length Myo10, but not coexpression of eGFP alone, suppressed nuclear displacement by the tail construct (Fig. 4b).

The oocyte nucleus is asymmetrically positioned by microtubules that extend from its surface to the F-actin rich cortical cytoskeleton[5,18]. Consequently, microtubule depolymerization in both amphibian and mammalian oocytes results in nuclear displacement, as the nucleus is less dense than the surrounding cytoplasm[5,6] (Fig. 4a). Thus, it was possible that disruption of Myo10 function resulted in microtubule depolymerization. However, although expression of the dominant negative tails mimicked the phenotype produced by microtubule depolymerization (Fig. 4a), they did so without causing microtubule depolymerization, as judged by both immunofluorescence analysis and biochemical quantification of polymeric tubulin (Supplementary Fig. S5).

As an independent means to test the *in vivo* role of Myo10, oocytes were microinjected with the affinity-purified Myo10 antibody. Anti-Myo10 microinjection resulted in the same phenotype as the dominant negative Myo10 tail expression, causing germinal vesicle displacement (Fig. 4c). This effect was both dose-dependent and specific, in that microinjection of a non-specific IgG failed to result in germinal vesicle displacement (Fig. 4c). Thus, Myo-10 is required for microtubule-dependent, asymmetric anchoring of the germinal vesicle.

Meiotic spindle assembly and/or positioning are F-actin dependent in oocytes[3,7,8,11]. To assess the potential role of Myo10 in spindle assembly, oocytes injected with either dominant negative Myo10 tail or anti-Myo10 antibodies were induced to undergo meiotic maturation by treatment with progesterone. The dominant negative Myo10 tail construct targeted to spindles (Supplementary Fig. S6) and the plasma membrane (data not shown) and this construct, as well as microinjection of Myo10 antibodies, severely impaired meiotic spindle assembly (Fig. 4d–f). The phenotypes produced, ranging from rotation failure and abnormal spindle structure, to multiple microtubule organizing centres (Figs 4d; Supplementary Fig. S7), mimic those previously described that result from actin depolymerization during meiotic maturation[7]. However, neither the Myo10 tail nor microinjection of Myo10 antibody resulted in actin disassembly. Rather, these manipulations resulted in abnormal F-actin–spindle association such that F-actin concentrated in aggregates on or near spindles or abortive microtubule organizing centres (Fig. 4d), indicating that Myo10 is essential for proper F-actin–meiotic spindle association. Thus, Myo10 disruption produced phenotypes characteristic of microtubule disassembly (nuclear displacement) or F-actin disassembly (failed spindle assembly) without disassembling either polymer system, indicating that this actin-based motor serves to link the microtubule and cortical F-actin cytoskeletons.

The identification of Myo10 as an essential integrator of micro-

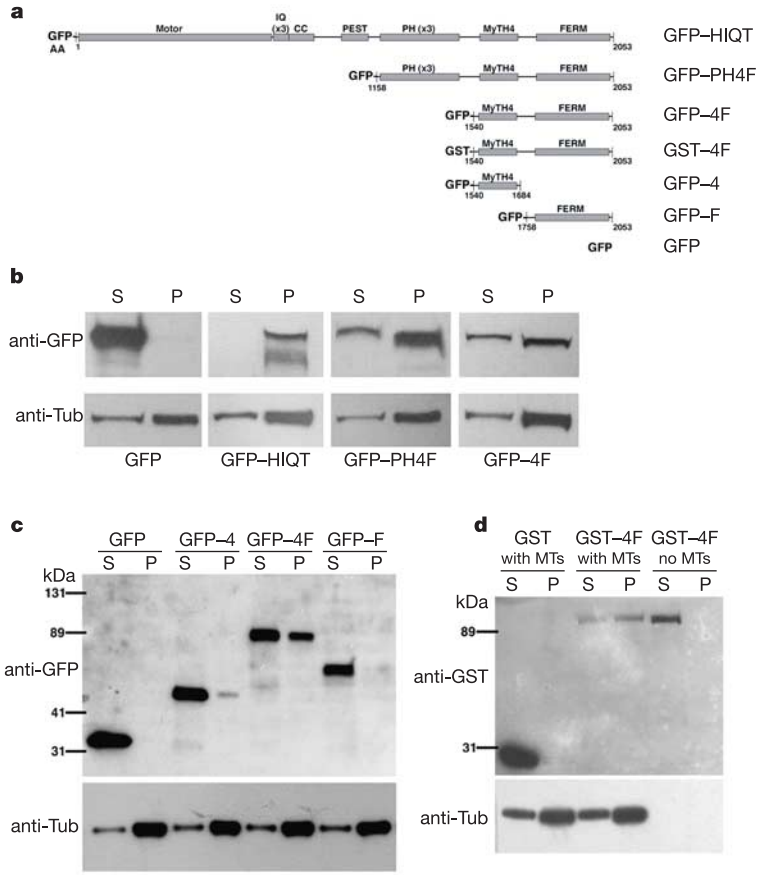

Figure 3 The MyTH4-FERM domain cassette of Myo10 binds microtubules. **a**, Constructs used for experiments in Figs 3 and 4. **b**, Immunoblot of the co-sedimentation assay shows that constructs containing the MyTH4 and FERM domains expressed through mRNA injection co-pellet with oocyte microtubules. **c**, Immunoblot of the co-sedimentation assay showing that both MyTH4 and FERM are required for optimal microtubule association in reticulocyte lysate. **d**, Immunoblot showing that GST–MyTH4-FERM but not GST purified following oocyte expression bind purified microtubules.

©2004 Nature Publishing Group

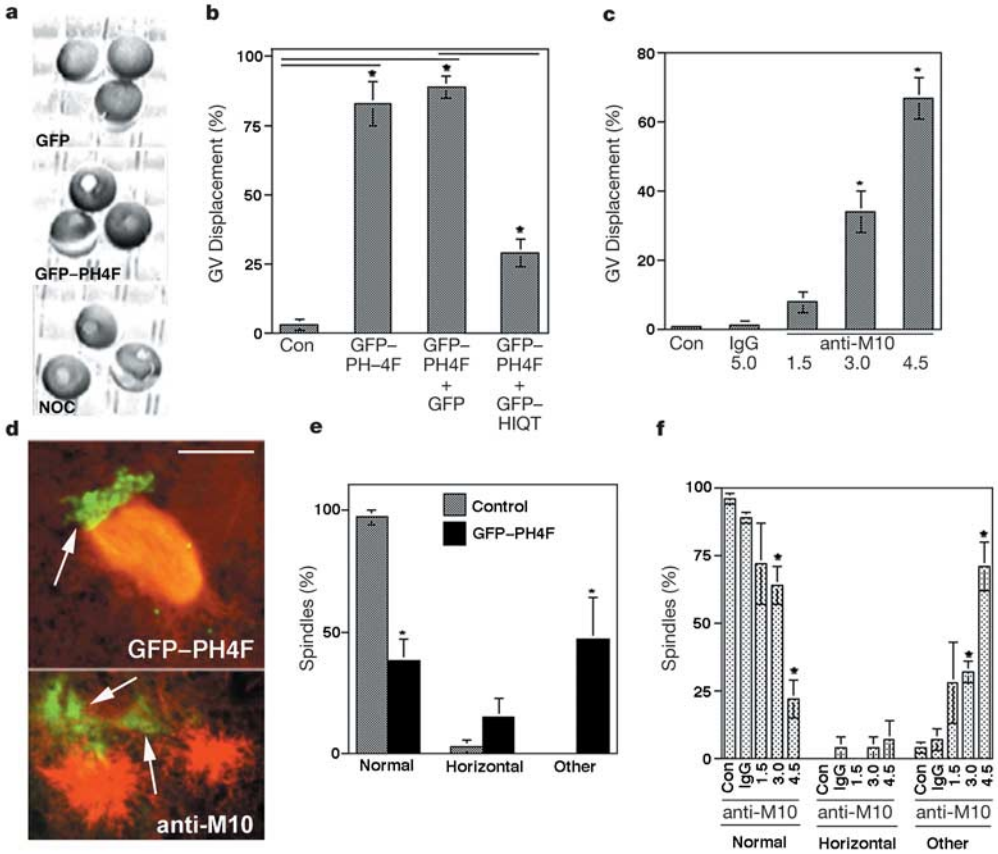

Figure 4 Myo10 is required for nuclear anchoring and meiotic spindle assembly. **a**, GFP–PH4F expression results in nuclear (germinal vesicle, GV) displacement in oocytes (shown by the white spot) not seen in controls that expressed GFP alone. Nocodazole (NOC) produced the same phenotype. **b**, The germinal vesicle displacement phenotype is suppressed by co-expression of GFP–HIQT but not GFP alone. **c**, Microinjection of the Myo10 antibody (M10) at increasing concentrations (numbers indicate concentration in needle, mg ml^{-1}) also resulted in germinal vesicle displacement. Non-specific IgG (IgG) had no effect. Lines above the bars indicate groups compared for statistical analysis. **d**, In egg expressing dominant negative Myo10 (cGFP–PH4F, upper panel), F-actin (pseudocoloured green) is found in aggregate (arrow) at one end of an unrotated, malformed spindle (red). In egg microinjected with anti-Myo10 antibody (M10, lower panel), two aberrant microtubule arrays (red) are present; F-actin (green) is in aggregates (arrows). Scale bar, 15 μm. **e**, GFP–PH4F expression impairs meiotic spindle assembly. **f**, Myo10 antibody also significantly impairs spindle assembly. Results are mean ± s.e.m. Asterisk indicates $P < 0.05$.

tubules with cortical F-actin in nuclear anchoring and spindle assembly in oocytes fits well with its known properties. That is, the PH domain-dependent binding of phosphoinositides[9,19], actin-binding and motor activity[20], and microtubule binding (this study) could function both passively and actively: passively for nuclear anchoring, through a stable association of nuclear microtubules with the cortex, where both phosphoinositides and F-actin are abundant; actively for spindle assembly, wherein the motor activity could be harnessed to help transport microtubule-associated spindle components over large distances. In addition, given the known association of myosin-10 with dynamic actin in other systems[10,17], an intriguing possibility is that the meiotic spindle cap may be composed of rapidly assembling actin and that myosin-10 could directly contribute to its assembly, through its association with Mena/VASP[21]. It will therefore be of great interest to determine whether association of myosin-10 with its various binding partners is differentially regulated, and whether such associations impact its motor activity.

This report has a further, critical implication. Namely, the demonstration that the Myo10 MyTH4-FERM domain cassette binds microtubules directly suggests that this cassette in other unconventional myosins may serve the same function. Of particular interest is myosin-7a. Genetic defects in myosin-7a result in Usher syndrome in humans[22], and myosin-7a localizes to cilia in a variety of tissues[23]. Because cilia are microtubule-rich, we suggest that this localization is mediated through the MyTH4-FERM domain of myosin-7a. More generally, our results, as well as demonstrations showing that other unconventional myosins can associate with microtubules indirectly[24,25] or directly[26] suggest that these motors may generally serve to integrate the F-actin and microtubule cytoskeletons. □

Methods

Oocyte culture, injection and immunofluorescence

Oocytes were obtained, microinjected and cultured as previously described[27]. For microtubule depolymerization, oocytes were incubated in culture medium containing 20 μM nocodazole for 24 h. Oocytes were analysed 24 h after antibody injection or 48 h after mRNA injection. For immunofluorescence, eggs were fixed and stained for F-actin and microtubules as previously described[28]. For extract experiments, immunofluorescence following rapid freezing was performed as described[29]. In both cases Myo10 antibody was used at 3 μg ml^{-1}.

Construct generation and expression

A small fragment of Myo10 was amplified by degenerate PCR[30] and full length sequence was obtained using 5′ and 3′ rapid amplification of cDNA ends (RACE). RNA was made as previously described using a pCS2-eGFP vector[27]. Oocytes were microinjected with 40 nl RNA at 1–4 mg ml^{-1} (needle concentration).

Antibody production and fractionation

Polyclonal antibodies against a fusion protein composed of GST and amino acids 269–390 of Myo10 were raised and affinity purified (after preclearing for GST-reactive antibodies). Prior to microinjection, antibodies were concentrated using microcon columns. For extracts, microtubule polymerization was induced or inhibited by addition of dimethylsulphoxide (DMSO) (20%) or nocodazole (20 μM), respectively, before pelleting and immunoblotting.

©2004 Nature Publishing Group

For reticulocyte lysate (Ambion) the manufacturer's instructions were followed for translation of added mRNA. Lysates were subjected to a 100,000*g* centrifugation to pellet insoluble material, and then the supernatants were combined with microtubules (assembled from purified tubulin) and pelleted by centrifugation at 100,000*g*. For expression and purification of GST and GST–MyTH4-FERM in oocytes, two days after injection, 75 oocytes were homogenized in PBS supplemented with protease inhibitors and 1% triton X-100. After a 5,000*g* clearing centrifugation, supernatants were mixed with glutathione–sepharose (Amersham) and incubated at 4 °C for 1 h. Glutathione–sepharose was then extracted 3 × with 1 M NaCl in PBS to remove any proteins associated with the constructs, and eluted with 10 mM glutathione. Eluates were pooled and concentrated with microcon columns, and then combined with microtubules assembled from purified tubulin. Microtubule fractions were then pelleted by a 100,000*g* centrifugation.

Received 6 March; accepted 12 July 2004; doi:10.1038/nature02834.

1. Gundersen, G. G. & Bretscher, A. Cell biology. Microtubule asymmetry. *Science* **300,** 2040–2041 (2003).
2. Rodriguez, O. C. *et al.* Conserved microtubule–actin interactions in cell movement and morphogenesis. *Nature Cell Biol.* **5,** 599–609 (2003).
3. Sardet, C., Prodon, F., Dumollard, R., Chang, P. & Chenevert, J. Structure and function of the egg cortex from oogenesis through fertilization. *Dev. Biol.* **241,** 1–23 (2002).
4. Lessman, C. A. Germinal vesicle migration and dissolution in *Rana pipiens* oocytes: effect of steroids and microtubule poisons. *Cell Differ.* **20,** 239–251 (1987).
5. Gard, D. L. Ectopic spindle assembly during maturation of *Xenopus* oocytes: evidence for functional polarization of the oocyte cortex. *Dev. Biol.* **159,** 298–310 (1993).
6. Alexandre, H., Van Cauwenberge, A. & Mulnard, J. Involvement of microtubules and microfilaments in the control of the nuclear movement during maturation of mouse oocyte. *Dev. Biol.* **136,** 311–320 (1989).
7. Gard, D. L., Cha, B. J. & Roeder, A. D. F-actin is required for spindle anchoring and rotation in *Xenopus* oocytes: a re-examination of the effects of cytochalasin B on oocyte maturation. *Zygote* **3,** 17–26 (1995).
8. Sun, Q. Y. *et al.* Dynamic events are differently mediated by microfilaments, microtubules, and mitogen-activated protein kinase during porcine oocyte maturation and fertilization *in vitro*. *Biol. Reprod.* **64,** 879–889 (2001).
9. Isakoff, S. J. *et al.* Identification and analysis of PH domain-containing targets of phosphatidylinositol 3-kinase using a novel *in vivo* assay in yeast. *EMBO J.* **17,** 5374–5387 (1998).
10. Berg, J. S., Derfler, B. H., Pennisi, C. M., Corey, D. P. & Cheney, R. E. Myosin-X, a novel myosin with pleckstrin homology domains, associates with regions of dynamic actin. *J. Cell Sci.* **113,** 3439–3451 (2000).
11. Kim, N.-H. *et al.* The distribution and requirements of microtubules and microfilaments in bovine oocytes during *in vitro* maturation. *Zygote* **8,** 25–32 (2000).
12. Shimizu, T. Polar body formation in *Tubifex* eggs. *Ann. NY Acad. Sci.* **582,** 260–272 (1990).
13. Sardet, C., Speksnijder, J., Terasaki, M. & Chang, P. Polarity of the ascidian egg cortex before fertilization. *Development* **115,** 221–237 (1992).
14. Sokac, A. M. & Bement, W. M. Regulation and expression of metazoan unconventional myosins. *Int. Rev. Cytol.* **200,** 197–304 (2000).
15. Narasimhulu, S. B. & Reddy, A. S. N. Characterization of microtubule binding domains in the *Arabidopsis* kinesin-like calmodulin binding protein. *Plant Cell* **10,** 957–965 (1998).
16. Rogers, S. L. *et al.* Regulation of melanosome movement in the cell cycle by reversible association with myosin V. *J. Cell Biol.* **146,** 1265–1276 (1999).
17. Cox, D. *et al.* Myosin-X is a downstream effector of PI(3)K during phagocytosis. *Nature Cell Biol.* **4,** 469–477 (2002).
18. Gard, D. L. Organization, nucleation, and acetylation of microtubules in *Xenopus laevis* oocytes: a study by confocal immunofluorescence microscopy. *Dev. Biol.* **143,** 346–362 (1991).
19. Yonezawa, S. *et al.* Possible involvement of myosin-X in intercellular adhesion: importance of serial pleckstrin homology regions for intracellular localization. *Dev. Growth Differ.* **45,** 175–185 (2003).
20. Homma, K., Saito, J., Ikebe, R. & Ikebe, M. Motor function and regulation of myosin X. *J. Biol. Chem.* **276,** 34348–34354 (2001).
21. Tokuo, H. & Ikebe, M. Myosin-X transports Mena/VASP to the tip of filapodia. *Biochem. Biophys. Res. Commun.* **319,** 214–220 (2004).
22. Weil, D. *et al.* Defective myosin VIIA gene responsible for Usher syndrome type 1B. *Nature* **374,** 60–61 (1995).
23. Wolfrum, U., Liu, X., Schmitt, A., Udovichenko, I. P. & Williams, D. S. Myosin VIIa as a common component of cilia and microvilli. *Cell. Motil. Cytoskeleton* **40,** 261–271 (1998).
24. Lantz, V. A. & Miller, K. G. A class VI unconventional myosin is associated with a homologue of a microtubule-binding protein, cytoplasmic linker protein-170, in neurons and at the posterior pole of *Drosophila* embryos. *J. Cell Biol.* **140,** 897–910 (1998).
25. Huang, J. D. *et al.* Direct interaction of microtubule- and actin-based transport motors. *Nature* **397,** 267–270 (1999).
26. Cao, T. T., Chang, W., Masters, S. E. & Mooseker, M. S. Myosin-Va binds to and mechanochemically couples microtubules to actin filaments. *Mol. Biol. Cell* **15,** 151–161 (2004).
27. Sokac, A. M., Co, C., Taunton, J. & Bement, W. Cdc42-dependent actin polymerization during compensatory endocytosis in *Xenopus* eggs. *Nature Cell Biol.* **5,** 727–732 (2003).
28. Mandato, C. A. & Bement, W. M. Actomyosin transports microtubules and microtubules control actomyosin recruitment during *Xenopus* oocyte wound healing. *Curr. Biol.* **13,** 1096–1105 (2003).
29. Weber, K. L. & Bement, W. M. F-actin serves as a template for cytokeratin organization in cell free extracts. *J. Cell Sci.* **115,** 1373–1382 (2002).
30. Bement, W. M., Hasson, T., Wirth, J. A., Cheney, R. E. & Mooseker, M. S. Identification and overlapping expression of multiple unconventional myosin genes in vertebrate cell types. *Proc. Natl Acad. Sci. USA* **91,** 6549–6553 (1994).

Supplementary Information accompanies the paper on **www.nature.com/nature**.

Acknowledgements Thanks to G. Von Dassow and J. Canman for critical reading of this manuscript. This work was supported by grants from the National Institutes of Health to W.M.B. and R.E.C.

Competing interests statement The authors declare that they have no competing financial interests.

Correspondence and requests for materials should be addressed to W.M.B. (wmbement@wisc.edu).

Pilus chaperones represent a new type of protein-folding catalyst

Michael Vetsch*, Chasper Puorger*, Thomas Spirig, Ulla Grauschopf, Eilika U. Weber-Ban & Rudi Glockshuber

Institut für Molekularbiologie und Biophysik, Eidgenössische Technische Hochschule Hönggerberg, CH-8093 Zürich, Switzerland

* These authors contributed equally to this work

Adhesive type 1 pili from uropathogenic *Escherichia coli* strains have a crucial role during infection by mediating the attachment to and potentially the invasion of host tissue. These filamentous, highly oligomeric protein complexes are assembled by the 'chaperone–usher' pathway[1], in which the individual pilus subunits fold in the bacterial periplasm and form stoichiometric complexes with a periplasmic chaperone molecule that is essential for pilus assembly[2–4]. The chaperone subsequently delivers the subunits to an assembly platform (usher) in the outer membrane, which mediates subunit assembly and translocation to the cell surface[5–8]. Here we show that the periplasmic type 1 pilus chaperone FimC binds non-native pilus subunits and accelerates folding of the subunit FimG by 100-fold. Moreover, we find that the FimC–FimG complex is formed quantitatively and very rapidly when folding of FimG is initiated in the presence of both FimC and the assembly-competent subunit FimF, even though the FimC–FimG complex is thermodynamically less stable than the FimF–FimG complex. FimC thus represents a previously unknown type of protein-folding catalyst, and simultaneously acts as a kinetic trap preventing spontaneous subunit assembly in the periplasm.

Type 1 pili from *E. coli* are composed of the main structural pilus subunit FimA, which forms the pilus rod, and subunits FimF, FimG and the adhesin FimH, which form the distal tip fibrillum[9] (Fig. 1). X-ray structures of chaperone–subunit and subunit–subunit complexes from different adhesive pilus systems have shown that pilus subunits have an immunoglobulin-like fold lacking a β-strand[10–13]. In chaperone–subunit complexes this incomplete fold of the pilus subunit is completed by a polypeptide segment of the chaperone, termed donor strand[10–13], whereas in the assembled pilus an amino-terminal extension of the adjacent pilus subunit acts as the donor strand[12–14] (Fig. 1).

On the basis of the above complementation principles, we designed an experiment that mimics pilus subunit folding in the periplasm. To test whether a folding subunit preferentially binds to the free chaperone or directly associates with the exposed donor strand of a chaperone-bound subunit, the chemically denatured subunit FimG was refolded in the presence of both the chaperone FimC and the subunit FimF. In order to inhibit self-polymerization of FimG and FimF, we used a FimG variant ($FimG_t$) lacking the 12 N-terminal donor strand residues, and a FimF variant ($FimF_F$) elongated at its carboxy terminus by a FimF donor strand that allows intramolecular donor strand complementation (see Supplementary Fig. S1). The only complexes that can form in this

©2004 Nature Publishing Group